Article

Structure Analyses of Dodecylated Single-Walled Carbon Nanotubes

Feng Liang, Lawrence B. Alemany, Jonathan M. Beach, and W. Edward Billups

J. Am. Chem. Soc., **2005**, 127 (40), 13941-13948• DOI: 10.1021/ja052870s • Publication Date (Web): 09 September 2005

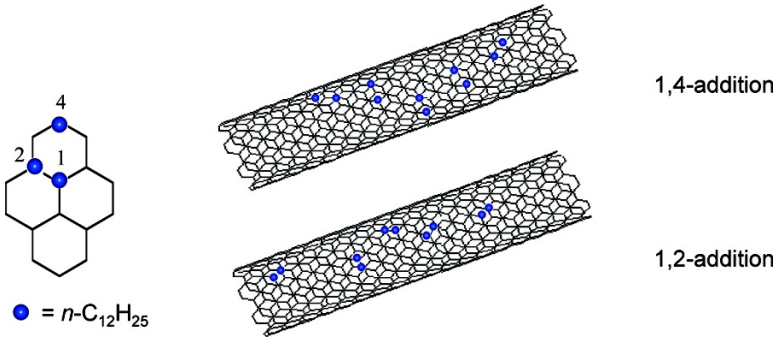

More About This Article

Additional resources and features associated with this article are available within the HTML version:

- Supporting Information
- Links to the 14 articles that cite this article, as of the time of this article download
- Access to high resolution figures
- Links to articles and content related to this article
- Copyright permission to reproduce figures and/or text from this article

View the Full Text HTML

J|A|C|S
ARTICLES
Published on Web 09/09/2005

Structure Analyses of Dodecylated Single-Walled Carbon Nanotubes

Feng Liang, Lawrence B. Alemany, Jonathan M. Beach, and W. Edward Billups*

Contribution from the Department of Chemistry and Center for Nanoscale Science and Technology, Rice University, Houston, Texas 77005

Received May 2, 2005; E-mail: billups@rice.edu

Abstract: Alkylation of nanotube salts prepared using either lithium, sodium, or potassium in liquid ammonia yields sidewall-functionalized nanotubes that are soluble in organic solvents. Atomic force microscopy and transmission electron microscopy studies of dodecylated SWNTs prepared from HiPco nanotubes and 1-iodododecane show that extensive debundling results from intercalation of the alkali metal into the SWNT ropes. TGA-FTIR analyses of samples prepared from the different metals revealed radically different thermal behavior during detachment of the dodecyl groups. The SWNTs prepared using lithium can be converted into the pristine SWNTs at 180−330 °C, whereas the dodecylated SWNTs prepared using sodium require a much higher temperature (380−530 °C) for dealkylation. SWNTs prepared using potassium behave differently, leading to detachment of the alkyl groups over the temperature range 180−500 °C. These differences can be observed by analysis of the solid-state ^{13}C NMR spectra of the dodecylated SWNTs that have been prepared using the different alkali metals and may indicate differences in the relative amounts of 1,2- and 1,4-addition of the alkyl groups.

Introduction

Among the wide range of nanometer scale structures prepared to date, single-walled carbon nanotubes (SWNTs) stand out as unique materials for fundamental research and emerging applications.[1,2] However, realistic applications have been hindered by difficulties associated with processing. SWNTs with a high degree of sidewall functionalization can, in principle, be used to overcome some of these difficulties because functionalized nanotubes may be soluble in organic solvents. Although impressive results have emerged from the flurry of activity in this area,[3] a more accommodating, efficient, and scalable approach is still desirable. Furthermore, uses in composites will require thermally robust functionalized SWNTs that will withstand the elevated temperatures required for many of the anticipated applications. We have observed previously that SWNTs can be reduced by lithium in liquid ammonia and the resulting nanotube salts can be reacted with alkyl iodides to yield debundled, functionalized SWNTs.[4] A mechanism to account for this observation is illustrated in the scheme illustrated below. Addition of an alkyl iodide to a suspension of SWNT salts results in the formation of a radical anion that dissociates readily into the alkyl radical and iodide. Addition of the radical to the debundled SWNTs leads to the functionalized nanotube.

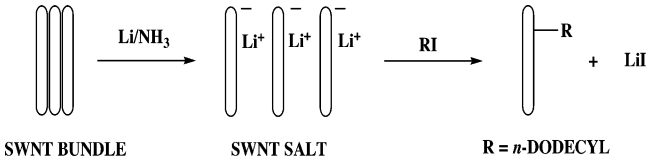

Thermal gravimetric analysis (TGA) of dodecylated SWNTs prepared using Li/NH_3 revealed that the alkyl groups detach

(1) Iijima, S.; Ichihashi, T. *Nature* **1993**, *363*, 603−605.
(2) (a) Tans, S. J.; Verschueren, A. R. M.; Dekker, C. *Nature* **1998**, *393*, 49−52. (b) Dai, H.; Wong, E. W.; Lieber, C. M. *Science* **1996**, *272*, 523−526. (c) Treacy, M. M. J.; Ebbesen, T. W.; Gibson, J. M. *Nature* **1996**, *381*, 678−680. (d) Wong, E. W.; Sheehan, P. E.; Lieber, C. M. *Science* **1997**, *277*, 1971−1975. (e) Poncharal, P.; Wang, Z. L.; Ugarte, D.; de Heer, W. A. *Science* **1999**, *283*, 1513−1516. (f) Yakobson, B. I.; Smalley, R. E. *Am. Sci.* **1997**, *85*, 324−337. (g) Calvert, P. *Nature* **1999**, *399*, 210−211. (h) Ajayan, P. M. *Chem. Rev.* **1999**, *99*, 1787−1799. (i) Baughman, R. H.; Zakhidov, A. A.; de Heer, W. A. *Science* **2002**, *297*, 787−792.
(3) (a) Mickelson, E. T.; Huffman, C. B.; Rinzler, A. G.; Smalley, R. E.; Hauge, R. H.; Margrave, J. L. *Chem. Phys. Lett.* **1998**, *296*, 188−194. (b) Chen, Y.; Haddon, R. C.; Fang, S.; Rao, A. M.; Eklund, P. C.; Lee, W. H.; Dickey, E. C.; Grulke, E. A.; Pendergrass, J. C.; Chavan, A.; Haley, B. E.; Smalley, R. E. *J. Mater. Res.* **1998**, *13*, 2423−2431. (c) Bahr, J. L.; Yang, J.; Kosynkin, D. V.; Bronikowski, M. J.; Smalley, R. E.; Tour, J. M. *J. Am. Chem. Soc.* **2001**, *123*, 6536−6542. (d) Georgakilas, V.; Tagmatarchis, N.; Pantarotto, D.; Bianco, A.; Briand, J.-P.; Prato, M. *Chem. Commun.* **2002**, 3050−3051. (e) Georgakilas, V.; Kordatos, K.; Prato, M.; Guldi, D. M.; Holzinger, M.; Hirsch, A. *J. Am. Chem. Soc.* **2002**, *124*, 760−761. (f) Pantarotto, D.; Partidos, C. D.; Graff, R.; Hoebeke, J.; Briand, J.-P.; Prato, M.; Bianco, A. *J. Am. Chem. Soc.* **2003**, *125*, 6160−6164. (g) Chen, J.; Hamon, M. A.; Hu, H.; Chen, Y.; Rao, A. M.; Eklund, P. C.; Haddon, R. C. *Science* **1998**, *282*, 95−98. (h) Holzinger, M.; Vostrowsky, O.; Hirsch, A.; Hennrich, F.; Kappes, M.; Weiss, R.; Jellen, F. *Angew. Chem., Int. Ed.* **2001**, *40*, 4002−4005. (i) Hu, H.; Zhao, B.; Hamon, M. A.; Kamaras, K.; Itkis, M. E.; Haddon, R. C. *J. Am. Chem. Soc.* **2003**, *125*, 14893−14900. (j) Holzinger, M.; Abraham, J.; Whelan, P.; Graupner, R.; Ley, L.; Hennrich, F.; Kappes, M.; Hirsch, A. *J. Am. Chem. Soc.* **2003**, *125*, 8566−8580. (k) Ying, Y.; Saini, R. K.; Liang, F.; Sadana, A. K.; Billups, W. E. *Org. Lett.* **2003**, *5*, 1471−1473. (l) Coleman, K. S.; Bailey, S. R.; Fogden, S.; Green, M. L. H. *J. Am. Chem. Soc.* **2003**, *125*, 8722−8723. (m) Pekker, S.; Salvetat, J.-P.; Jakab, E.; Bonard, J.-M.; Forro, L. *J. Phys. Chem. B* **2001**, *105*, 7938−7943. (n) Sun, Y.-P.; Huang, W.; Lin, Y.; Fu, K.; Kitaygorodskiy, A.; Riddle, L. A.; Yu, Y. J.; Carroll, D. L. *Chem. Mater.* **2001**, *13*, 2864−2869. (o) Peng, H.; Reverdy, P.; Khabashesku, V. N.; Margrave, J. L. *Chem. Commun.* **2003**, 362−363. (p) Peng, H.; Alemany, L. B.; Margrave, J. L.; Khabashesku, V. N. *J. Am. Chem. Soc.* **2003**, *125*, 15174−15182 and references therein.

thermally at 180−330 °C, temperatures too low for many of the anticipated applications. More recently, we have observed that nanotube salts prepared using either Na/NH_3 or K/NH_3 may be functionalized by alkyl iodides to yield materials that exhibit radically different thermal behavior, suggesting that the alkylation step is highly dependent on the metal cation. SWNTs functionalized by *n*-dodecyl groups are amenable to characterization by solid-state[5] ^{13}C NMR spectroscopy. In this paper, we report characterizations of dodecylated SWNTs prepared with different alkali metals, their disparate thermal behavior, and discuss differences in terms of 1,2- versus 1,4-addition to the nanotube framework.

Experimental Section

Materials. The raw SWNTs used in this study were produced at Rice University by the HiPco process.[6] The average diameter of the SWNTs was around 1 nm. The iron nanoparticles, coated by carbon, were removed by a multistep oxidation at increasing temperatures in the presence of SF_6 followed by a Soxhlet extraction with a 6 M HCl solution as described previously.[7] The iron residue in the purified SWNTs was determined to be ∼6 wt % by TGA.

Lithium (granules, 99%), sodium (cube, 99.95%, in mineral oil), potassium (rod, diameter 25 mm, 99.5%, in mineral oil), and 1-iodododecane were purchased from Aldrich.

Synthetic Procedure. The functionalization reactions were carried out as follows: 20 mg (1.6 mmol of carbon) of SWNTs was added to a flame dried 100 mL three neck round-bottom flask. NH_3 (60 mL) was then condensed into the flask followed by the addition of small pieces of alkali metal (8.0 mmol). The 1-iodododecane (1.90 g, 6.4 mmol) was then added, and the reaction mixture was stirred overnight with the slow evaporation of NH_3. The flask was then cooled in an ice bath as methanol (10 mL) was added slowly followed by water (20 mL). After acidification (10% HCl), the nanotubes were extracted into hexanes and washed several times with water. The hexane layer was then filtered through a 0.2 μm PTFE membrane filter, washed with ethanol and chloroform, and dried in a vacuum oven (80 °C) overnight.

Characterization. The dodecylated SWNTs were characterized by Raman spectroscopy, TGA-FTIR, AFM, TEM, and solid-state ^{13}C NMR. Raman spectra were collected from solid samples, using a Renishaw 1000 micro-Raman system with a 780 nm laser source. The thermal degradation studies were carried out using a SDT 2960 Simultaneous DSC-TGA from TA Instruments. The gaseous species released from the sample during pyrolysis were fed into the FT-IR spectrometer, and concentrations of the thermally detached radicals were monitored with time and temperature. Atomic force microscopy (AFM) was performed with a Digital Instruments Nanoscope IIIa in tapping mode using a 3045 JVW piezo tube scanner. Transmission electron microscopy (TEM) images were obtained from JEOL 2010F operating at 100 kV.

The solid-state, magic angle spinning (MAS) NMR studies were done on a Bruker AVANCE-200 NMR spectrometer (50.3 MHz ^{13}C, 200.1 MHz ^{1}H) described previously.[3p] Each sample was packed into a 4 mm outer diameter rotor. Chemical shifts are reported relative to the carbonyl carbon of glycine defined as 176.46 ppm.[8] To facilitate comparing spectra for a given experiment among the three samples, the same parameters were used for each sample (except for small variations in the number of scans).

The basic $^{1}H-^{13}C$ CPMAS spectra were obtained with 7 kHz MAS, a 1-ms contact time, 29.3-ms FID, and 5-s relaxation delay. The spectral range (extending from δ457 to δ−237) was sufficient for detecting spinning sidebands at ±7 and ±14 kHz. Li/NH_3 product, 33 240 scans; Na/NH_3 product, 31 720 scans; K/NH_3 product, 34 400 scans; empty rotor, 49 400 scans. Preliminary spectra of the dodecylated SWNTs were also obtained with 5 kHz MAS.

The dipolar dephasing experiments differed only in that after CP two equal dephasing periods with a 180° ^{13}C refocusing pulse in the middle were used before FID acquisition. Li/NH_3 product: 33 640 scans and a pair of 20-μs dephasing periods, or a pair of 25-μs dephasing periods, or a pair of 30-μs dephasing periods. Na/NH_3 product: 31 720 scans and a pair of 25-μs dephasing periods, or a pair of 30-μs dephasing periods, or a pair of 40-μs dephasing periods. K/NH_3 product: 34 400 scans and a pair of 25-μs dephasing periods.

The direct ^{13}C pulse spectra were obtained with 11 kHz MAS, a 4.5-μs 90° ^{13}C pulse, 20.53-ms FID, and 10-s relaxation delay. The spectral range (extending from δ607 to δ−387) was sufficient for detecting spinning sidebands at ±11 and ±22 kHz. Li/NH_3 or Na/NH_3 or K/NH_3 products, 10 400 scans; empty rotor, 2544 scans. After phase correction, a fourth-order polynomial was applied to the baseline over the region from δ230 to δ−70 to create a nearly flat baseline after the polynomial was subtracted from the spectrum of the dodecylated SWNTs. For the Li/NH_3 sample, the experiment was repeated with a 30-s relaxation delay. The resulting spectrum was essentially superimposable on that obtained with just a 10-s relaxation delay, and therefore the Na/NH_3 and K/NH_3 samples were studied with only a 10-s relaxation delay.

Each FID of dodecylated SWNTs was processed with 50 Hz (1 ppm) of line broadening. None of the FIDs for the dodecylated SWNTs were truncated.

The model compounds *n*-$C_{24}H_{50}$ and 1,4-didodecylbenzene were studied with the same CP and dipolar dephasing parameters to allow direct comparison with the dodecylated SWNTs except as follows. Far fewer scans were needed: 96 scans for *n*-$C_{24}H_{50}$ and 144 scans for 1,4-didodecylbenzene. In the dipolar dephasing experiment, pairs of 5-μs, 10-μs, 15-μs, 20-μs, 25-μs, 30-μs, and 40-μs dephasing delays were used to more carefully determine the time needed for the CH_2 and CH signals to decay. Only 5 Hz (0.1 ppm) of line broadening was used to process a FID. The sinc wiggles in the spectra of the model compounds (Figures S-2 and S-3) result from truncated FIDs.

Results and Discussion

Raman Spectroscopy. Raman spectra of solid samples prepared using the three metals are presented in Figure 1. The unresolved tangential mode (G band) of the SWNTs appears as a strong peak at ∼1590 cm^{-1} with a shoulder at ∼1560 cm^{-1}. The radial breathing modes that show multiple peaks near ∼230 cm^{-1} are related to the diameters of the nanotubes. The disorder mode (D band) centered at ∼1290 cm^{-1} is widely used as a measure of covalent sidewall derivatization. The low intensity of the D band in the starting material (Figure 1a) indicates a very low level of initial sidewall functionalization or damage to the purified SWNTs used in this study. The large D bands that emerged after functionalization with Li/NH_3, Na/NH_3, and K/NH_3 (Figure 1b,c,d, respectively) demonstrate the high degree of functionalization achieved during these alkylation reactions. The Na/NH_3 product shows the largest D to G ratio, indicating that sodium provides the highest degree of functionalization.

Microscopy. The dodecylated SWNTs prepared from nanotube salts by reduction with Na/NH_3 and K/NH_3 exhibit high solubility in chloroform, THF, and DMF, as observed earlier

(4) Liang, F.; Sadana, A. K.; Peera, A.; Chattopadhyay, J.; Gu, Z.; Hauge, R. H.; Billups, W. E. *Nano Lett.* **2004**, *4*, 1257−1260.
(5) Characterization of these materials by solution-state NMR spectroscopy is not possible because solutions are too dilute and the functionalized SWNTs tumble too slowly and anisotropically in solution to allow for adequate characterization by NMR spectroscopy, especially ^{13}C NMR spectroscopy.
(6) Bronikowski, M. J.; Willis, P. A.; Colbert, D. T.; Smith, K. A.; Smalley, R. E. *J. Vac. Sci. Technol., A* **2001**, *19*, 1800−1805.
(7) Xu, Y.; Peng, H.; Hauge, R. H.; Smalley, R. E. *Nano Lett.* **2005**, *5*, 163−168.
(8) Hayashi, S.; Hayamizu, K. *Bull. Chem. Soc. Jpn.* **1991**, *64*, 685−687.

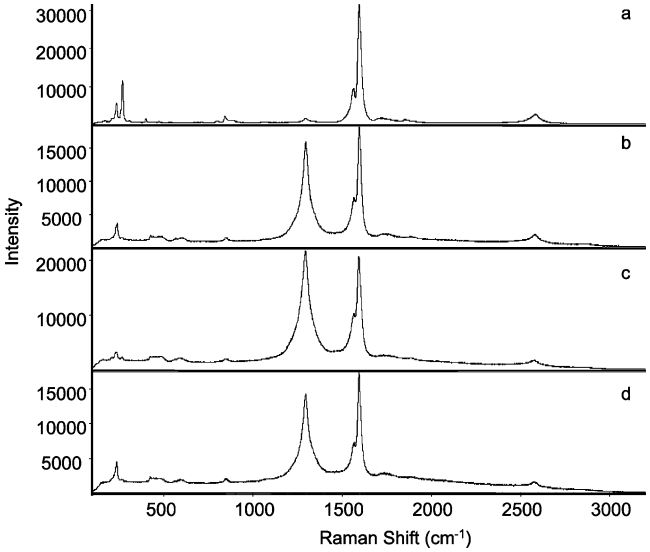

Figure 1. Raman spectra of (a) pristine SWNTs, and SWNTs dodecylated by (b) Li/NH_3 reduction, (c) Na/NH_3 reduction, and (d) K/NH_3 reduction.

for SWNTs functionalized by Li/NH_3.[4] Atomic force microscopy (AFM) images recorded in chloroform for each sample are presented in Figure 2. The average diameters of the dodecylated SWNTs in both cases are around 2 nm as determined by their height, demonstrating that extensive debundling has occurred. Additional evidence for debundling is provided by inspection of the HRTEM images presented in Figure 3. The dodecylated SWNTs exhibit a morphology that is expected for functionalized nanotubes.

Thermal Gravimetric Analysis. Although the Raman spectra and microscopy studies are not informative with respect to the nature of the products that result from the various metals, TGA analyses revealed radically different thermal behavior as the alkyl groups detach from the SWNTs (Figure 4). These experiments were carried out in the furnace of an apparatus coupled to an FT-IR spectrometer. The samples were held at 80 °C for 30 min, ramped 10 °C min^{-1} to 800 °C, and then held at 800 °C for 10 min. The gaseous species released from the sample during the pyrolysis were introduced into the FT-IR spectrometer, and concentration variations during the pyrolysis process were monitored with time and temperature. The dodecylated SWNTs prepared using Li/NH_3 (trace a) exhibit a major peak between 180 and 330 °C, and a smaller peak at ~480 °C. In contrast, dodecylated SWNTs prepared using Na/NH_3 (trace b) produce a quite different profile: a minor peak between 180 and 280 °C and a major peak between 380 and 530 °C, indicating that dodecylated SWNTs prepared using sodium as the reducing agent lead to the more thermally robust materials. For the sample prepared using K/NH_3 (trace c), two peaks of similar intensity at two different temperature regions were observed. The weight loss indicates that there is one dodecyl group for every 24, 13, and 25 nanotube carbons in the Li/NH_3, Na/NH_3, and K/NH_3 products, respectively.

In Figure 5, the chemigram of the Na/NH_3 sample is shown along with the derivative weight loss curve. The similar shapes of these curves demonstrate that the gaseous species exhibiting the aliphatic C−H stretching in the 3000−2800 cm^{-1} range account for the observed weight loss, providing further evidence that the SWNTs have been dodecylated. Similar derivative weight loss curves for the Li/NH_3 and K/NH_3 samples are nearly identical to their respective chemigrams.

Solid-State ^{13}C NMR Spectroscopy. The disparate thermal behavior of the SWNTs functionalized with the different alkali metals can be rationalized in terms of the relative amounts of 1,2- and 1,4-addition[9] of alkyl groups to the SWNTs as shown by ^{13}C NMR spectroscopy.

The first indication by NMR that the SWNTs were significantly changed upon dodecylation was shown by our ability to spin any of the dodecylated SWNTs at the desired speed and to tune easily the ^{13}C and ^{1}H channels of the probe. In marked contrast, the rotor containing the pristine SWNTs with ~6 wt % iron would not spin above about 2 kHz, and the probe would not tune properly. Differences in the NMR spectra of dodecylated SWNTs prepared using Li/NH_3, Na/NH_3, and K/NH_3 are evident from comparing the three direct ^{13}C pulse MAS spectra (Figures 6a, 7a, and 8a), the three $^{1}H-^{13}C$ CPMAS spectra (Figures 6b, 7b, and 8b), and the three $^{1}H-^{13}C$ CPMAS spectra with a dephasing delay before FID acquisition (Figures 6c, 7c, and 8c). The expected qualitative features are observed in the spectra for each of the samples: The basic CPMAS spectrum discriminates against carbons far from protons; inserting an appropriate dephasing delay in the CPMAS experiment eliminates the methylene carbon signals and, based on the remaining relatively strong signal near $\delta 30$, causes considerably faster decay of the methyl carbon signals than of the quaternary aliphatic carbons signals.

Of particular interest are the aliphatic carbon signals in the CPMAS experiments with a 1-ms contact time followed by a dipolar dephasing period of 50 μs (Figures 6c, 7c, and 8c). These aliphatic signals are noteworthy because these signals can be attributed only to quaternary aliphatic carbons,[10] that is, the nanotube sp^2 carbons that became sp^3 carbons upon dodecylation, and to methyl carbons[10] terminating the dodecyl chains. Furthermore, the differences in signal shape and intensity of the three samples prepared using a different alkali metal show that the metal chosen affects the reductive alkylation process, as it is the only variable in the three reactions. This observation is consistent with the different Raman and TGA-FTIR spectra obtained when Li/NH_3, Na/NH_3, and K/NH_3 were used.

The aliphatic carbon NMR signal in the experiments with 50-μs dephasing times provides direct evidence for the alkylation of the SWNTs in addition to the evidence provided by the appearance of the Raman signal near 1290 cm^{-1} for sp^3 carbon. The ^{13}C NMR signals from the various dodecyl methylene carbons would be expected to be weak, at most, with a dephasing time of 40 μs and nulled or even slightly inverted with a dephasing time of 50 μs.[10] The Li/NH_3 product was also studied with dephasing times of 40 and 60 μs, while the Na/NH_3 product was also studied with dephasing times of 60 and 80 μs. In all three cases with dephasing times of at least 60 μs, the aliphatic carbon signal remained (albeit less intense than

(9) Kelly, K. F.; Chiang, I. W.; Mickelson, E. T.; Hauge, R. H.; Margrave, J. L.; Wang, X.; Scuseria, G. E.; Radloff, C.; Halas, N. J. *Chem. Phys. Lett.* **1999**, *313*, 445−450. Nanoscale images (STM) of fluorinated SWNTs reveal a banded structure that indicates broad continuous regions of fluorination terminating in bands orthogonal to the tube axis. Although theoretical calculations indicated that the energy differences between the 1,2- and 1,4-isomers are small at all levels of fluorination, the 1,4-isomer was found to be slightly more stable.

(10) (a) Opella, S. J.; Frey, M. H. *J. Am. Chem. Soc.* **1979**, *101*, 5854−5856. (b) Alemany, L. B.; Grant, D. M.; Alger, T. D.; Pugmire, R. J. *J. Am. Chem. Soc.* **1983**, *105*, 6697−6704.

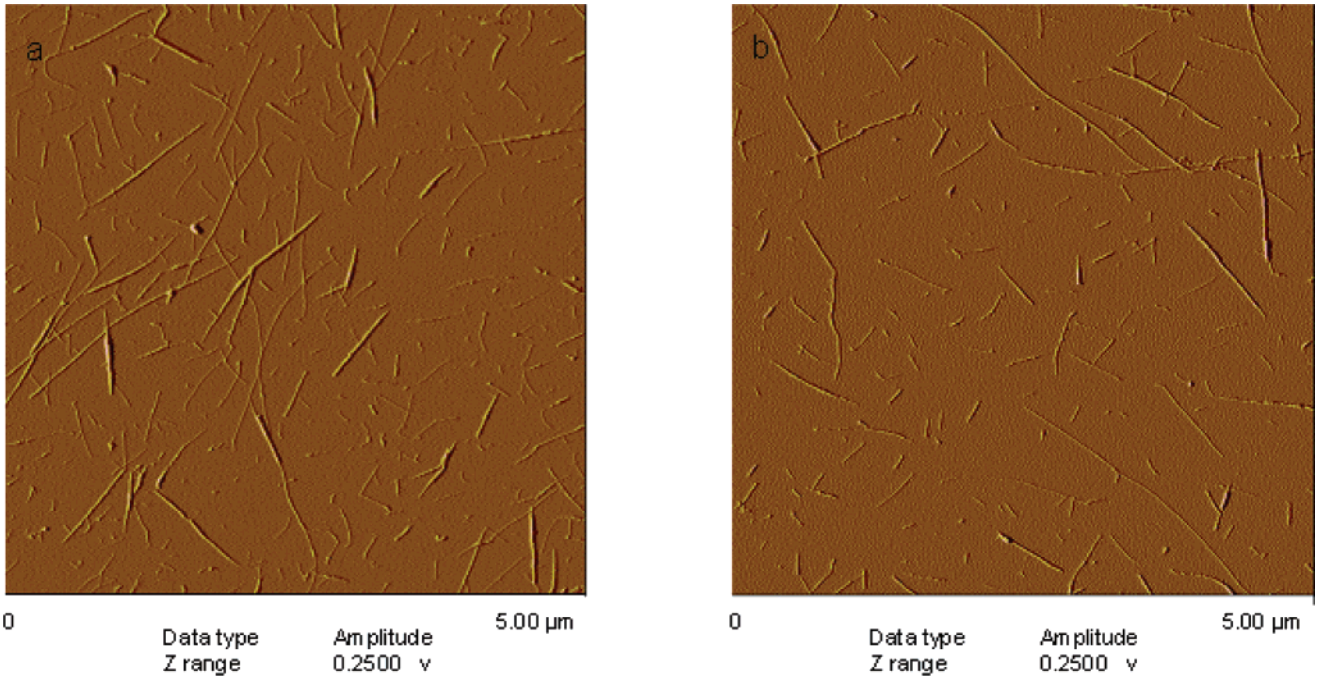

Figure 2. Tapping mode AFM images of *n*-dodecylated SWNTs spin-coated from chloroform: (a) Na/NH_3 reduction, (b) K/NH_3 reduction.

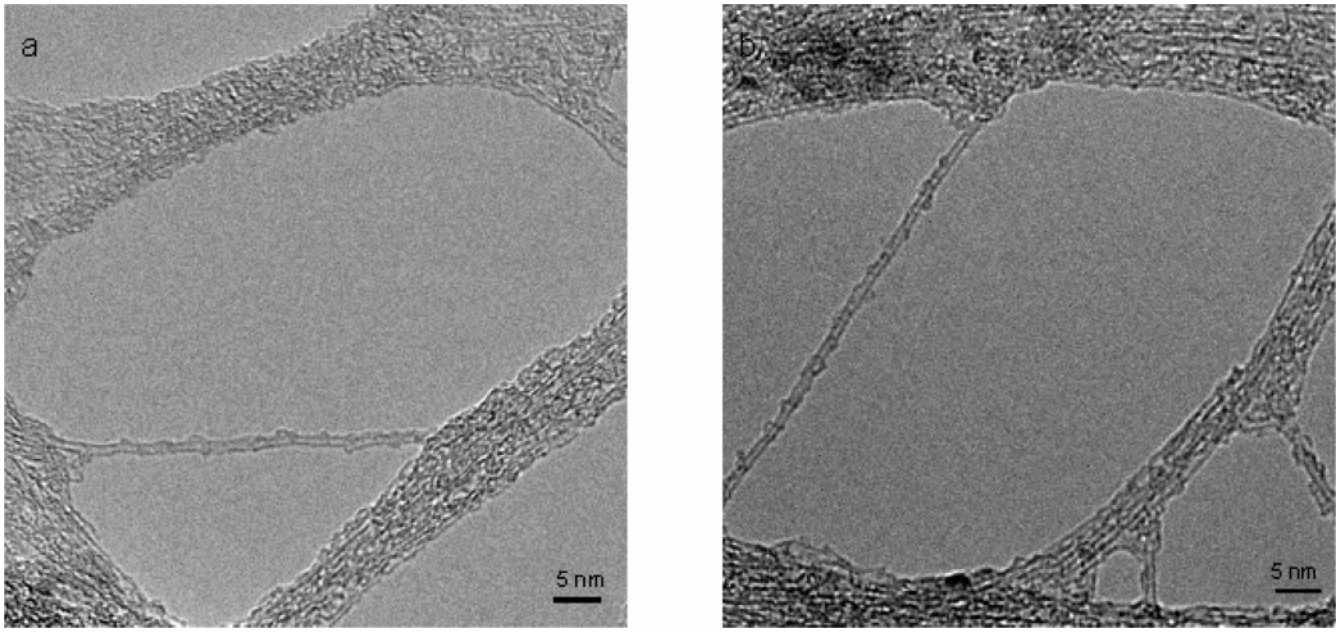

Figure 3. HRTEM images of *n*-dodecylated SWNTs that were functionalized by (a) Na/NH_3 reduction, and (b) K/NH_3 reduction.

with a dephasing time of only 50 μs), which strengthens the interpretation of this signal as principally arising from quaternary aliphatic carbons. [The K/NH_3 product gave a weak aliphatic carbon signal with a dephasing time of 50 μs (Figure 8c); therefore, studying this sample with a longer dephasing time did not seem worthwhile.] The experiments on the Na/NH_3 product with dephasing times of 50, 60, and 80 μs showed that the quaternary aliphatic signal decayed faster than the nanotube sp^2 carbon signal (Supporting Information, Figure S-1), which is reasonable[10] because every quaternary aliphatic carbon is adjacent to protons on a methylene group.

Dipolar dephasing studies on two model compounds with long alkyl groups (n-$C_{24}H_{50}$ and 1,4-didodecylbenzene) show the expected rapid decay of the CH_2 signals (Supporting Information, Figures S-2 and S-3). With a dephasing delay of 40 μs, significant CH_3 and substituted aromatic carbon signals remain, as expected, while the signal for the interior carbons of the methylene chain has just begun to invert. With a dephasing delay of 50 μs, the inversion is more noticeable. With a dephasing delay of 60 μs, the continuing dipolar modulation causes the CH_2 signal to be less negative until, with a dephasing delay of 80 μs, the CH_2 signal is not detectable above the noise, and only significant positive CH_3 and (with 1,4-didodecylbenzene) substituted aromatic carbon signals remain. n-$C_{24}H_{50}$ was chosen for study because it is a significant byproduct of the reductive alkylation reaction;[4] therefore, this compound cannot be contributing to the aliphatic signal observed in the dipolar dephasing spectra shown in Figures 6c, 7c, and 8c. In contrast, 1,4-

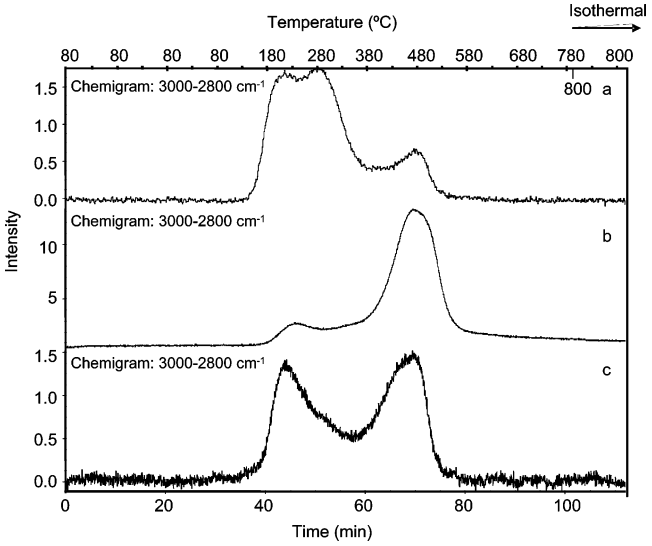

Figure 4. Chemigram of *n*-dodecylated SWNTs that were functionalized by three different alkali metals: (a) lithium, (b) sodium, and (c) potassium. TGA weight loss %: (a) 37, (b) 53, and (c) 36.

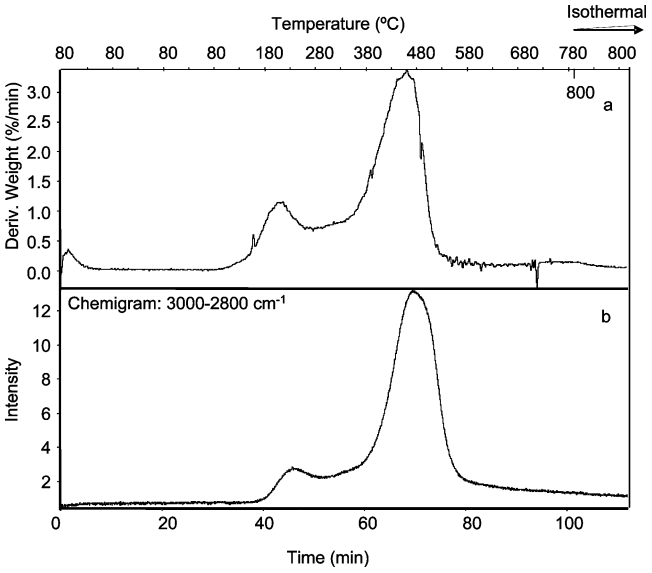

Figure 5. Correlation of the TGA derivative weight percentage curve (a) and the chemigram of the gaseous species (b) released from the *n*-dodecylated SWNTs prepared by Na/NH_3 reduction. (Temperature profile: 30 min hold at 80 °C, ramp 10 °C min^{-1} to 800 °C, 10 min hold at 800 °C). The slight lag (~2 min) of the C−H signal is due to the time it takes the released gases to reach the IR detector.

didodecylbenzene was chosen for study only because it was a simple, commercially available compound with dodecyl groups. The dipolar dephasing data on these two compounds with long alkyl groups show that using a dephasing delay of 50 μs is sufficient for obtaining spectra showing just nanotube sp^2 carbons, quaternary aliphatic carbons, and methyl carbons in the samples of dodecylated SWNTs. (With such complex samples, any weakly inverted CH_2 signals are completely obscured by the much more slowly decaying quaternary aliphatic carbon signals.) Indeed, using a 50-μs dephasing delay severely attenuates the upfield part of the aliphatic carbon signal from each of the dodecylated SWNTs.

With MAS at 7 kHz and no nanotube sp^2 carbon signal visible above the noise downfield of δ140 in the dipolar dephasing spectra (Figures 6c, 7c, and 8c), the aliphatic carbon signal in

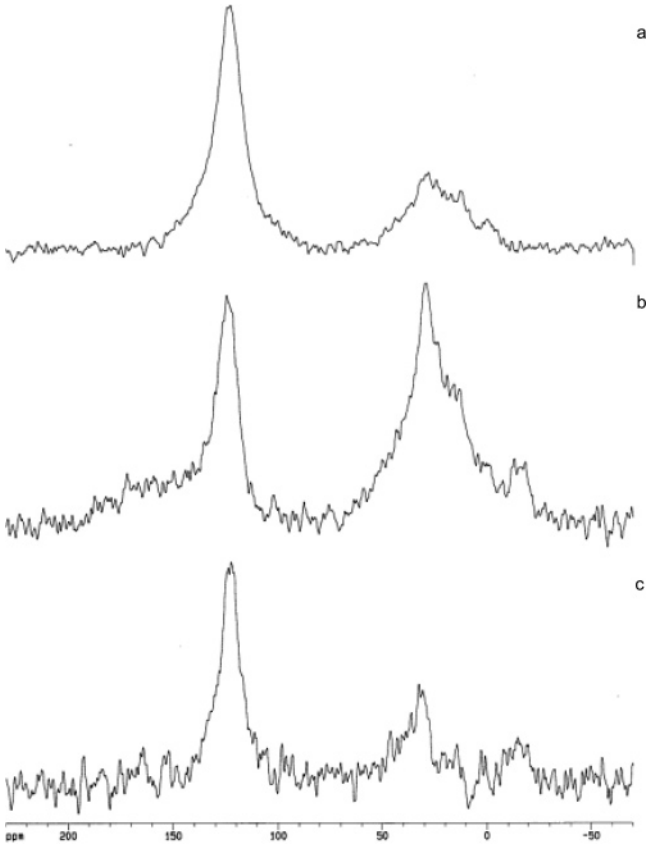

Figure 6. Dodecylated SWNTs prepared by Li/NH_3 reductive alkylation with n-$C_{12}H_{25}I$: (a) direct ^{13}C pulse MAS spectrum, (b) $^1H-^{13}C$ CPMAS spectrum, and (c) $^1H-^{13}C$ CPMAS spectrum with a 50-μs dephasing delay before FID acquisition.

these spectra does not contain intensity from an upfield spinning sideband of the nanotube sp^2 carbon signals. At this spinning speed, the first upfield spinning sideband of the nanotube sp^2 carbon signals is at about $\delta-16$ (i.e., 139 ppm upfield of the centerband). This spinning sideband is very weak and well upfield of the aliphatic carbon centerband signals in Figures 6c, 7c, and 8c. (The broad downfield tail in the sp^2 region in Figures 6b, 7b, and 8b apparently results from either probe background, the zirconia rotor barrel, or the Kel-F rotor cap, as obtaining a CPMAS spectrum of an empty rotor under the same conditions used for the dodecylated SWNTs gave a very weak, very broad signal in the sp^2 region.)

The signals from the methyl carbon terminating the long alkyl chain would be expected to be only partially attenuated with 50-μs to 80-μs dephasing times[10] and to appear near δ14. In the Li/NH_3 product, these signals are visible only in the experiment with the 40-μs dephasing period. Even the quaternary aliphatic carbon signal intensity is strongly attenuated with a 60-μs dephasing time. The S/N in the dipolar dephasing spectrum of the K/NH_3 product is too low to allow the methyl signals to be detected. In contrast, with the Na/NH_3 product, the signal intensity near δ14 is noticeable, even with an 80-μs dephasing period.

It was not feasible to obtain spectra with significantly higher S/N or to perform experiments with additional dephasing times because each dipolar dephasing experiment required 44−48 h with a full 4 mm rotor.

Quaternary aliphatic carbons exhibiting different chemical shifts are to be expected because the starting material is a

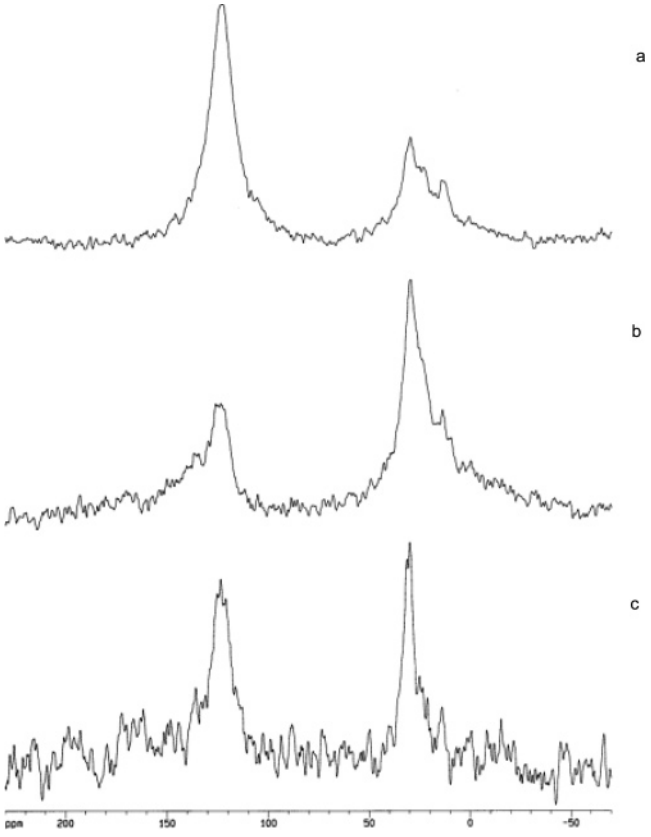

Figure 7. Dodecylated SWNTs prepared by Na/NH_3 reductive alkylation with *n*-$C_{12}H_{25}I$: (a) direct ^{13}C pulse MAS spectrum, (b) $^1H-^{13}C$ CPMAS spectrum, and (c) $^1H-^{13}C$ CPMAS spectrum with a 50-μs dephasing delay before FID acquisition.

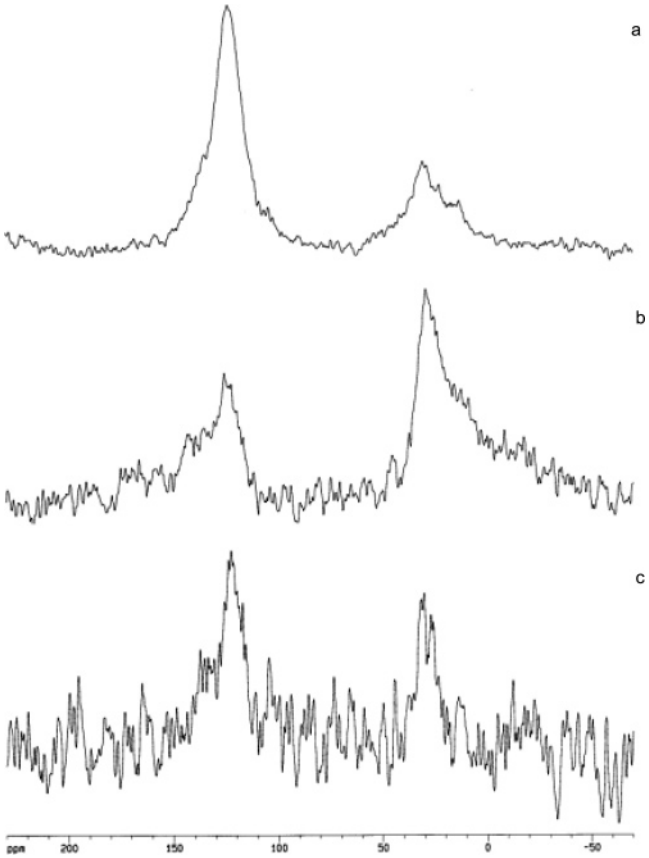

Figure 8. Dodecylated SWNTs prepared by K/NH_3 reductive alkylation with *n*-$C_{12}H_{25}I$: (a) direct ^{13}C pulse MAS spectrum, (b) $^1H-^{13}C$ CPMAS spectrum, and (c) $^1H-^{13}C$ CPMAS spectrum with a 50-μs dephasing delay before FID acquisition.

complex mixture of SWNTs differing in diameter and chirality and because alkylation is expected to occur at different nanotube sites and with different substitution patterns. The chemical shift range for the quaternary aliphatic carbons generated upon dodecylation indicates that these carbons more closely resemble those in dialkyldihydro derivatives of large planar condensed aromatic hydrocarbons than the quaternary aliphatic carbons in the analogous derivatives of the highly curved fullerenes C_{60} and C_{70}. Such chemical shifts for the quaternary aliphatic carbons of the dodecylated SWNTs are reasonable, because the SWNTs are less curved than C_{60} or C_{70}[3p] and because chemical shift is very sensitive to changes in bond lengths and bond angles.[11] That C_{60} molecules fit inside SWNTs like peas in a pod[12] is perhaps the most graphic illustration of the much higher curvature of C_{60}.

In contrast to the signals commonly found from about δ55−65 for the quaternary aliphatic carbons of alkylated C_{60} and C_{70},[13−16] signals are commonly found from δ30−40 for the interior quaternary aliphatic carbons of dialkyldihydro derivatives of planar condensed aromatic hydrocarbons (including those with only alkyl substituents on the periphery). Many NMR studies have been reported for dialkyldihydro derivatives of pyrene and numerous derivatives formed by annelating various aromatic ring systems onto pyrene.[17] Compounds with these extended aromatic ring systems are relevant in analyzing the ^{13}C chemical shifts of the dodecylated SWNTs. (Background

(11) (a) Grant, D. M. *Encyclopedia of Nuclear Magnetic Resonance*; Wiley: London, 1996; Vol. 2, pp 1298−1321. (b) Nossal, J.; Saini, R. K.; Sadana, A. K.; Bettinger, H. F.; Alemany, L. B.; Scuseria, G. E.; Billups, W. E.; Saunders, M.; Khong, A.; Weisemann, R. *J. Am. Chem. Soc.* **2001**, *123*, 8482−8495.

(12) Vostrowsky, O.; Hirsch, A. *Angew. Chem., Int. Ed.* **2004**, *43*, 2326−2329 and references therein.

(13) (a) Caron, C.; Subramanian, R.; D'Souza, F.; Kim, J.; Kutner, W.; Jones, M. T.; Kadish, K. M. *J. Am. Chem.* Soc. **1993**, *115*, 8505−8506. (b) Allard, E.; Rivière, L.; Delaunay, J.; Dubois, D.; Cousseau, J. *Tetrahedron Lett.* **1999**, *40*, 7223−7226. (c) Al-Matar, H.; Abdul Sada, A. K.; Avent, A. G.; Taylor, R.; Wei, X.-W. *J. Chem. Soc., Perkin Trans. 2* **2002**, 1251−1256.

(14) (a) Wang, G.-W.; Murata, Y.; Komatsu, K.; Wan, T. S. M. *Chem. Commun.* **1996**, 2059−2060. (b) Allard, E.; Rivière, L.; Delaunay, J.; Rondeau, D.; Dubois, D.; Cousseau, J. *Proc.-Electrochem. Soc.* **2000**, *2000-10*, 88−93. (c) Allard, E.; Delaunay, J.; Cousseau, J. *Org. Lett.* **2003**, *5*, 2239−2242.

(15) (a) Abdul-Sada, A. K.; Avent, A. G.; Birkett, P. R.; Kroto, H. W.; Taylor, R.; Walton, D. R. M. *J. Chem. Soc., Perkin Trans. 1* **1998**, 393−395. (b) Meier, M. S.; Bergosh, R. G.; Gallagher, M. E.; Spielmann, H. P.; Wang, Z. *J. Org. Chem.* **2002**, *67*, 5946−5952.

(16) (a) Kadish, K. M.; Gao, X.; Van Caemelbecke, E.; Hirasaka, T.; Suenobu, T.; Fukuzumi, S. *J. Phys. Chem. A* **1998**, *102*, 3898−3906. (b) Fukuzumi, S.; Suenobu, T.; Hirasaka, T.; Arakawa, R.; Kadish, K. M. *J. Am. Chem. Soc.* **1998**, *120*, 9220−9227. (c) Kadish, K. M.; Gao, X.; Van Caemelbecke, E.; Suenobu, T.; Fukuzumi, S. *J. Phys. Chem. A* **2000**, *104*, 3878−3883. (d) Allard, E.; Delaunay, J.; Cousseau, J. *Org. Lett.* **2003**, *5*, 2239−2242. (e) Toganoh, M.; Suzuki, K.; Udagawa, R.; Hirai, A.; Sawamura, M.; Nakamura, E. *Org. Biomol. Chem.* **2003**, *1*, 2604−2611. (f) Wang, G.-W.; Zhang, T.-H.; Wang, F. *Org. Biomol. Chem.* **2004**, *2*, 1160−1163. (g) Matsuo, Y.; Nakamura, E. *J. Am. Chem. Soc.* **2005**, *127*, 8457−8466.

(17) (a) Du Vernet, R.; Boekelheide, V. *Proc. Natl. Acad. Sci. U.S.A.* **1974**, *71*, 2961−2964. (b) Yamamoto, K.; Ueda, T.; Yumioka, H.; Okamoto, Y.; Yoshida, T. *Chem. Lett.* **1984**, 1977−1978. (c) Mitchell, R. H.; Iyer, V. S.; Khalifa, N.; Mahadevan, R.; Venugopalan, S.; Weerawarna, S. A.; Zhou, P. *J. Am. Chem. Soc.* **1995**, *117*, 1514−1532, 5168. (d) Mitchell, R. H.; Iyer, V. S. *J. Am. Chem. Soc.* **1996**, *118*, 2903−2906. (e) Lai, Y.-H.; Zhou, Z.-L. *J. Org. Chem.* **1997**, *62*, 925−931. (f) Mitchell, R. H.; Zhang, J. *Tetrahedron Lett.* **1997**, *38*, 6517−6520. (g) Bodwell, G. J.; Bridson, J. N.; Chen, S.-L.; Poirier, R. A. *J. Am. Chem. Soc.* **2001**, *123*, 4704−4708. (h) Williams, R. V.; Armantrout, J. R.; Twamley, B.; Mitchell, R. H.; Ward, T. R.; Bandyopadhyay, S. *J. Am. Chem. Soc.* **2002**, *124*, 13495−13505. (i) Mitchell, R. H.; Ward, T. R.; Chen, Y.; Wang, Y.; Weerawarna, S. A.; Dibble, P. W.; Marsella, M. J.; Almutairi, A.; Wang, Z.-Q. *J. Am. Chem. Soc.* **2003**, *125*, 2974−2988. (j) References to other work cited in these papers.

information for various aspects of the NMR analysis is provided in the Supporting Information.) For ^{13}C NMR data of a model compound to be relevant for interpreting the spectra of dodecylated SWNTs, the quaternary aliphatic carbons of the model have to occupy interior ring positions, for example, the 10b and 10c positions of pyrene:

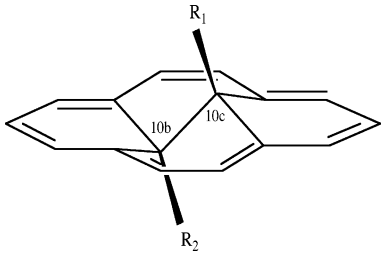

1a: $R_1 = R_2 = CH_3$
1b: $R_1 = R_2 = C_2H_5$
1c: $R_1 = R_2 = n\text{-}C_3H_7$
1d: $R_1 = n\text{-}C_{11}H_{23}$, $R_2 = CH_3$

Quaternary aliphatic carbons on the periphery of the ring system, ^{13}C NMR data for which have been reported for a few derivatives of pyrene[18a,b] and one derivative of perylene,[18c] are not very useful models.

All of the literature ^{13}C NMR data for dialkyldihydro derivatives of pyrene and larger planar condensed aromatic hydrocarbons appear to be for compounds bearing alkyl groups at adjacent sites (e.g., the 10b and 10c positions in pyrene), analogous to 1,2-addition in a fullerene. Unfortunately, almost all of these data are for compounds where the alkyl groups are trans to one another, as the cis compounds are much less common.[17c,g,19] In dodecylated SWNTs, all of the alkyl groups are on the exterior, that is, cis to one another. So the starting point for the NMR analysis is the only *cis*-dialkyldihydro derivative of a large planar condensed aromatic hydrocarbon for which quaternary aliphatic carbon chemical shift data appear to have been reported:[17g]

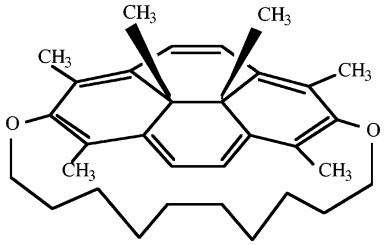

2

The $-O(CH_2)_{10}O-$ tether in **2** was critical for generating the *cis*-dimethyl stereochemistry in the synthesis and does not impose any strain on the ring system.[20] On the basis of the reported spectrum and shift data,[17g] we conclude that the signal at δ33.9 results from the quaternary aliphatic carbon.

It now becomes necessary to estimate the quaternary aliphatic carbon chemical shift upon replacing the methyl groups with dodecyl groups. Replacing the methyl groups with *n*-propyl groups would be expected to deshield the quaternary aliphatic carbon by 5 ppm in light of the chemical shift for the quaternary aliphatic carbon in *trans*-10b,10c-dimethyl-10b,10c-dihydropyrene (**1a**, δ30.0) and *trans*-10b,10c-dipropyl-10b,10c-dihydropyrene (**1c**, δ34.9).[17a] As would be expected,[21,22] the methyl group terminating the propyl chain exerts a negligible γ-shielding effect on the quaternary aliphatic carbon, as this carbon gives a signal at δ35.1 in *trans*-10b,10c-diethyl-10b,10c-dihydropyrene (**1b**).[17a] Lengthening the propyl chain would introduce δ- and longer range effects that would be expected to affect the quaternary aliphatic carbon chemical shift by much less than 1 ppm. Thus, one might estimate that replacing the methyl groups in **2** with dodecyl groups would deshield the quaternary aliphatic carbons by about 5 ppm so that the signal would be at about δ39. The center of the quaternary aliphatic carbon signal is near δ39 in the dipolar dephasing spectrum of the Li/NH_3-generated dodecylated SWNTs (Figure 6c), which suggests that 1,2-addition to a bond shared by two six-membered rings is significant.

The quaternary aliphatic carbons in the dodecylated SWNTs prepared by Na/NH_3 reduction and K/NH_3 reduction are more shielded than those prepared by Li/NH_3 reduction. This *might* be an indication of considerably more 1,4- than 1,2-addition in the Na/NH_3- and K/NH_3-generated dodecylated SWNTs in light of the data in Table S-1 (Supporting Information), which show that the quaternary aliphatic carbon of a 1,4-disubstituted C_{60} derivative with two identical CH_2Z groups gives a signal 7−15 ppm upfield of the quaternary aliphatic carbon in the corresponding 1,2-disubstituted C_{60} derivative. Indeed, as discussed in the Supporting Information, in the di- and higher substituted derivatives of C_{60} and C_{70}, 1,4-addition appears to be more common than 1,2-addition.

Dodecylating a complex mixture of SWNTs differing in diameter and chirality results in a range of quaternary aliphatic carbon environments differing from one another. An obvious difference is 1,2-addition to a bond shared by two six-membered rings versus 1,4-addition across a six-membered ring (Figure S-4). More subtle differences arise from the same type of addition to SWNTs differing in diameter and chirality so that small but significant differences in bond angles and bond distances exist in the environment of the quaternary aliphatic carbons. A range of quaternary aliphatic carbon chemical shifts then results because, as noted earlier, chemical shift is very sensitive to bond lengths and bond angles.

In any event, in a standard $^1H-^{13}C$ CP experiment the significant quaternary aliphatic signal intensity near δ30 in the Na/NH_3 and K/NH_3 products is completely obscured by the signals for the numerous interior CH_2 carbons that would also

(18) (a) Hempenius, M. A.; Erkelens, C.; Mulder, P. P. J.; Zuilhof, H.; Heinen, W.; Lugtenburg, J.; Cornelisse, J. *J. Org. Chem.* **1993**, *58*, 3076−3084. (b) van Dijk, J. T. M.; Lugtenburg, J.; Cornelisse, J. *J. Chem. Soc., Perkin Trans. 2* **1995**, 1489−1495. (c) Ebert, L. B.; Milliman, G. E.; Mills, D. R.; Scanlon, J. C. *Adv. Chem. Ser.* **1988**, *217*, 109−126.

(19) (a) Mitchell, R. H.; Boekelheide, V. *J. Chem. Soc. D: Chem. Commun.* **1970**, 1555−1557. (b) Kamp, D.; Boekelheide, V. *J. Org. Chem.* **1978**, *43*, 3475−3477. (c) Mitchell, R. H.; Mahadevan, R. *Tetrahedron Lett.* **1981**, *22*, 5131−5134. (d) Mitchell, R. H.; Chaudhary, M.; Kamada, T.; Slowey, P. D.; Williams, R. V. *Tetrahedron* **1986**, *42*, 1741−1744. (e) Mitchell, R. H.; Bodwell, G. J.; Vinod, T. K.; Weerawarna, K. S. *Tetrahedron Lett.* **1988**, *29*, 3287−3290. (f) Lai, Y.-H.; Zhou, Z.-L. *J. Org. Chem.* **1994**, *59*, 8275−8278.

(20) Bodwell, G. J.; Bridson, J. N.; Chen, S.-L.; Li, J. *Eur. J. Org. Chem.* **2002**, 243−249.

(21) Wehrli, F. W.; Wirthlin, T. *Interpretation of Carbon-13 NMR Spectra*; Heyden: London, 1976; p 28.

(22) Another example of the negligible γ-shielding effect upon a quaternary aliphatic carbon is provided by the chemical shifts for C-3 of 3,3-dimethylheptane (δ32.62) and for C-4 of 4,4-dimethyloctane (δ32.66) (obtained in dilute solutions in $CDCl_3$; unpublished data).

give a signal near δ30.[17e] This makes the usefulness of the dipolar dephasing experiment particularly apparent. Simpler spectra should result from methylation. With no methylene signals present, the dipolar dephasing experiment should not be necessary.

For the three samples, comparing the intensity of the aliphatic signal among the basic CPMAS spectra or among the dipolar dephasing spectra shows that the intensity is the highest for the Na/NH_3 product. This parallels what is observed for the intensity of the 1290 cm^{-1} band in the Raman spectra of the dodecylated products. These NMR and Raman results are consistent with the TGA results, indicating significantly more dodecylation in the Na/NH_3 reaction (one dodecyl chain for every 13 nanotube carbons) than in the Li/NH_3 or K/NH_3 reactions (one dodecyl chain for every 24 or 25 nanotube carbons, respectively). For the Na/NH_3 product, it is not obvious if there is a common explanation for the relatively simple TGA profile (exhibiting a major high temperature decomposition peak from detachment of the dodecyl groups) and the relatively sharp aliphatic carbon signal in the basic CPMAS and dipolar dephasing NMR spectra. It is also apparent from the relatively low S/N in the basic CPMAS and dipolar dephasing spectra of the K/NH_3 product that this material did not undergo CP as efficiently as the Li/NH_3 and Na/NH_3 products, again demonstrating the subtle influence that the choice of metal has on the reductive dodecylation reaction.

Conclusion

Addition of alkyl iodides to carbon nanotube salts prepared with lithium, sodium, or potassium yields highly functionalized SWNTs that exhibit distinct thermal behavior as demonstrated by thermal gravimetric analysis. These differences can be observed by analysis of the solid-state ^{13}C NMR spectra of the dodecylated SWNTs that have been prepared with the different alkali metals and may indicate differences in the relative amounts of 1,2- and 1,4-addition of the alkyl groups.

Acknowledgment. We thank the Robert A. Welch Foundation (C-0490), Texas Advanced Technology Program (003604-0113-2003), DARPA (ONR-20041018), and the National Science Foundation (CHE-0450085) for support of this work. We also thank the Office of Naval Research (N00014-96-1-1146) for purchase of the 200 MHz NMR spectrometer.

Supporting Information Available: $^{1}H-^{13}C$ CPMAS spectra of dodecylated SWNTs prepared by Na/NH_3 reductive alkylation and two model compounds (*n*-$C_{24}H_{50}$ and 1,4-didodecylbenzene) with various dephasing delays before FID acquisition. Relevant background information for various aspects of the NMR analysis. This material is available free of charge via the Internet at http://pubs.acs.org.

JA052870S